

## Translation Rate of Human Tyrosinase Determines Its N-Linked Glycosylation Level\*

Received for publication, October 9, 2000, and in revised form, November 3, 2000  
Published, JBC Papers in Press, November 7, 2000, DOI 10.1074/jbc.M009203200

Andrea Újvári<sup>‡§</sup>, Rebecca Aron<sup>‡§</sup>, Thomas Eisenhaure<sup>‡</sup>, Elaine Cheng<sup>¶</sup>, Hadas A. Parag<sup>‡</sup>,  
Yoel Smicun<sup>¶</sup>, Ruth Halaban<sup>¶</sup>, and Daniel N. Hebert<sup>‡¶</sup>

From the <sup>‡</sup>Department of Biochemistry and Molecular Biology, Program in Molecular and Cellular Biology, University of Massachusetts, Amherst, Massachusetts 01003 and the <sup>¶</sup>Department of Dermatology, Yale University School of Medicine, New Haven, Connecticut 06520

Tyrosinase is a type I membrane glycoprotein essential for melanin synthesis. Mutations in tyrosinase lead to albinism due, at least in part, to aberrant retention of the protein in the endoplasmic reticulum and subsequent degradation by the cytosolic ubiquitin-proteasomal pathway. A similar premature degradative fate for wild type tyrosinase also occurs in amelanotic melanoma cells. To understand critical cotranslational events, the glycosylation and rate of translation of tyrosinase was studied in normal melanocytes, melanoma cells, an *in vitro* cell-free system, and semi-permeabilized cells. Site-directed mutagenesis revealed that all seven N-linked consensus sites are utilized in human tyrosinase. However, glycosylation at Asn-290 (Asn-Gly-Thr-Pro) was suppressed, particularly when translation proceeded rapidly, producing a protein doublet with six or seven N-linked core glycans. The inefficient glycosylation of Asn-290, due to the presence of a proximal Pro, was enhanced in melanoma cells possessing 2–3-fold faster (7.7–10.0 amino acids/s) protein translation rates compared with normal melanocytes (3.5 amino acids/s). Slowing the translation rate with the protein synthesis inhibitor cycloheximide increased the glycosylation efficiency in live cells and in the cell-free system. Therefore, the rate of protein translation can regulate the level of tyrosinase N-linked glycosylation, as well as other potential cotranslational maturation events.

Whereas prokaryotic proteins fold posttranslationally due to their rapid rate of translation, the maturation of nascent proteins in eukaryotic cells often begins cotranslationally as a vectorial process and continues posttranslationally after the release of the protein from the ribosome (1–4). The slower rate of protein translation observed in eukaryotic cells has been proposed to play an important role in the proper folding of proteins in the cell by permitting the sequential folding of individual domains during the translation process (5). Understanding how proteins acquire their native structure in the cell is of fundamental significance. Because key protein maturation

events for eukaryotic cells occur cotranslationally and have a large impact on the fidelity of the overall maturation process, it is important to fully understand these cotranslational processes.

For proteins that traverse the secretory pathway, the cotranslational processes include the translocation of the protein across the endoplasmic reticulum (ER)<sup>1</sup> membrane, the site of entry into the secretory pathway. In this case, protein folding commences upon emergence of the polypeptide chain into the lumen of the ER. The ER is an organelle that specializes in the efficient folding, modification, and assembly of proteins to their native structures prior to their packaging into transport vesicles. The milieu of the ER is topologically equivalent to the extracellular space, with oxidizing conditions permitting the cotranslational and posttranslational formation of disulfide bonds (1, 6–9).

Additional covalent modifications in the ER include the transfer of N-linked core glycans to Asn residues found in the consensus sequence Asn-X-(Thr/Ser) (10). This transfer can occur cotranslationally after the Asn is 12–14 amino acids into the ER lumen, positioning it proximal to the active site of the oligosaccharyl transferase (OST) (1, 11). Immediately after its transfer, the glycan side chains are trimmed by glucosidases I and II, generating glycoproteins possessing monoglucosylated glycans that are substrates for the lectin chaperones calnexin and calreticulin (12–15). Release from the chaperones is then initiated after the cleavage of the third glucose by glucosidase II (14, 16). The binding of these lectin chaperones to their substrates promotes correct folding and oligomeric assembly (17–19). Thus, oligosaccharides play a central role in the quality control system of the ER that determines the fate of the maturing cargo glycoproteins (20–22).

Melanocytes are specialized cells dedicated to the production of melanin. Tyrosinase (monophenol, L-dopa:oxygen oxidoreductase, EC 1.14.18.1), is the key melanocyte-specific enzyme that catalyzes the oxidation of tyrosine and DOPA to DOPAquinone, and 5,6-dihydroxyindole to indole-5,6-quinone (23–25). The biosynthesis of melanin takes place in post-Golgi endomembranous compartments called melanosomes or pigmented granules. Mutational analysis of tyrosinase-positive albinism has identified AP-3 as an important protein involved

\* This work was supported by grants from the Medical Foundation, Edward Mallinckrodt, Jr. Foundation, and United States Public Health Service Grant CA79864 (to D. N. H.) and by United States Public Health Service Grants AR39848 (to R. H.) and AR41942 (Yale Skin Diseases Research Center; R. E. Tigelaar, Program Investigator). The costs of publication of this article were defrayed in part by the payment of page charges. This article must therefore be hereby marked "advertisement" in accordance with 18 U.S.C. Section 1734 solely to indicate this fact.

§ These authors contributed equally to this work.

¶ To whom correspondence should be addressed. E-mail: dhebert@biochem.umass.edu.

<sup>1</sup> The abbreviations used are: ER, endoplasmic reticulum; Azc, azetidine-2-carboxylic acid; CHX, cycloheximide; DNJ, deoxynojirimycin; GFP, green fluorescent protein; K<sup>b</sup>SS, murine major histocompatibility complex class I molecule K<sup>b</sup> signal sequence; OST, oligosaccharyl transferase; PAGE, polyacrylamide gel electrophoresis; RER, rough ER; RRL, rabbit reticulocyte lysate; TYR, human tyrosinase; TYR<sup>6</sup>, tyrosinase with 6 glycans; TYR<sup>7</sup>, tyrosinase with 7 glycans; <sup>125</sup>I-TYR, untranslocated tyrosinase; WG, wheat germ; CHAPS, 3-[3-(cholamidopropyl)dimethylammonio]-1-propanesulfonic acid.

in the sorting of tyrosinase in the *trans*-Golgi to melanosomes (26–28, reviewed in Ref. 29). However, additional key sorting decisions for tyrosinase are made in the early secretory pathway that are critical for pigmentation (30–32).

Tyrosinase is a membrane glycoprotein with an N-terminal signal sequence that targets the protein to the ER (Fig. 1A) (33–36). The human protein possesses 7 putative N-linked glycosylation sites and 15 luminal Cys residues that can participate in disulfide bond formation. Mutations in tyrosinase are the cause of tyrosinase-negative oculocutaneous albinism 1, an autosomal recessive genetic disorder characterized by the absence of melanin (reviewed in Refs. 37 and 38). The mutant protein in several tyrosinase-negative albino melanocytes of human and mouse origin is retained in the ER (31, 39). The essential role of the ER in the regulation of tyrosinase has also been demonstrated in amelanotic melanoma cells in which ER retention of wild type tyrosinase leads to subsequent degradation by the 26 S proteasome (30).

Here, we demonstrate that the faster rate of translation of tyrosinase in melanoma cells than that of normal melanocytes hampered glycosylation at the inefficient Asn-290 site. This was determined by studying tyrosinase glycosylation and maturation under conditions that altered the rate of translation in normal melanocytes and melanoma cells, as well as in a cell-free system that recapitulated the ER processes.

#### EXPERIMENTAL PROCEDURES

**Materials**—Rabbit reticulocyte lysate (RRL), wheat germ (WG), dithiothreitol, and RNasin were from Promega Corp. (Madison, WI). Canine pancreas microsomes were a generous gift from Dr. R. Gilmore (Worcester, MA). [<sup>35</sup>S]Methionine/cysteine (EasyTag) and CHAPS were from PerkinElmer Life Sciences and Pierce, respectively. Restriction endonucleases and ribonucleotide triphosphates were from New England Biolabs, Inc. (Beverly, MA).

mMessage mMachine and T7 transcription kits were from Ambion (Austin, TX), and the QuikChange site-directed mutagenesis kit was from Stratagene (La Jolla, CA). Zysorbin (fixed and killed *Staphylococcus aureus*) was obtained from Zymed Laboratories Inc. (San Francisco, CA). All other reagents, including the anti-FLAG M2 monoclonal antibody, were from Sigma.

**Construction of Plasmids Encoding Wild Type and Mutant Tyrosinase Proteins**—The plasmid pcTYR carrying the human tyrosinase gene (GenBank™ accession number Y00819) was a gift from Dr. R. Spritz (Denver, CO). The EcoRI tyrosinase fragment excised from pcTYR was subcloned into pGEM 7Zf (Promega). To improve *in vitro* translation/translocation, the original signal sequence of tyrosinase was exchanged with the murine major histocompatibility complex class I molecule K<sup>b</sup> signal sequence as follows. A XbaI restriction site was introduced at the end of the 18-amino acid signal sequence in pGEM 7Zf-TYR plasmid by site-directed mutagenesis (QuikChange site-directed mutagenesis kit, Stratagene). The tyrosinase XbaI fragment (encoding the full sequence of tyrosinase minus the signal peptide) was inserted into the XbaI restriction site of pSP72/K<sup>b</sup>SS-CD3δ plasmid (from Drs. J. Huppa and H. Ploegh, Boston, MA) (40). This created a hybrid molecule comprising the class I heavy chain H2-K<sup>b</sup> signal peptide in frame with the tyrosinase protein downstream of the T7 promoter, termed pSP72/K<sup>b</sup>SS-TYR.

To generate single-site glycosylation deletion mutant proteins, the consensus N-linked glycosylation sites Asn-X-Thr/Ser in pSP72/K<sup>b</sup>SS-TYR were eliminated or modified in the cDNA by changing threonine or serine to an alanine, except for Thr-373, which was changed to the albino mutation T373K. The site at Asn-290 was modified by exchanging the proline at position 293 to alanine (P293A). The P293A and T292A mutations were also introduced to tyrosinase cDNA in the enhanced green fluorescent protein (enhanced GFP) vector (31). In addition, the wild type and mutant cDNAs were subcloned from the enhanced GFP plasmids into the KpnI/HindII cloning sites of p3XFLAG-CMV-14 expression vector (Sigma) to generate FLAG-tagged tyrosinase proteins. In all cases, DNA sequencing of the entire tyrosinase gene verified the inserted mutations. Transfection of plasmids into mouse melanocytes was done as described (31).

**Transcription, Translation, and Translocation**—Messenger RNA was prepared by *in vitro* run-off transcription of the cDNA that was linearized with NdeI or HaeII, according to the manufacturer's instructions. Radioactive [<sup>35</sup>S]-labeled tyrosinase was translated for 1 h at 27 °C

in RRL (14) or in WG and translocated cotranslationally into canine pancreas microsomes. In the latter case, WG lysate (40 μl) was mixed with ribonuclease-treated rough ER (RER) microsomes (6 μl), an amino acid mixture lacking methionine and cysteine (6 μl of a 1 mM solution of each), [<sup>35</sup>S]Met/Cys (63 μCi), RNase-free water (18.4 μl), RNase inhibitor (1.6 μl), and mRNA (1 μg/μl, 3.5 μl). Samples were alkylated with N-ethylmaleimide (20 mM) to block free sulfhydryls (7). Alkylated samples were either analyzed directly by SDS-PAGE or immunoprecipitated with anti-tyrosinase antibodies (α-TYR) prior to electrophoresis. Deoxynojirimycin (DNJ) (0.5 mM) was used to inhibit ER glucosidases when indicated. Half of each sample was subjected to nonreducing SDS-PAGE, and the other half was reduced by the addition of dithiothreitol (100 mM) and resolved by reducing SDS-PAGE.

Semipermeabilized cells were prepared from subconfluent mouse B10BR melanocytes (41) permeabilized with 20 μg/ml digitonin using a method described previously by Wilson *et al.* (42). Radioactive [<sup>35</sup>S]-labeled tyrosinase was translated for 1 h at 27 °C in RRL with semipermeabilized cells (1.3 × 10<sup>4</sup> cells/μl) replacing the RER microsomes.

**Identification of Translocated Protein**—To separate glycosylated (TYR) from nonglycosylated (untranslocated (<sup>U</sup>TYR)) proteins, 10 μl of the translation mixture was solubilized in 200 μl of 2% CHAPS buffer (2% CHAPS, 50 mM HEPES, 200 mM sodium chloride, pH 7.5), and glycoproteins were captured on wheat germ agglutinin-bound beads at 4 °C for 2 h under constant rotation. The beads were pelleted by centrifugation at 2500 × g and washed once with 0.5% CHAPS buffer. The bound proteins were then eluted in SDS-sample buffer at 95 °C for 5 min. Alternatively, untranslocated tyrosinase was separated from the translocated protein by centrifugation of the translation products (10 μl) through a sucrose cushion (100 μl, 0.5 M sucrose, 50 mM triethanolamine, 1 mM dithiothreitol, pH 7.4) in a Beckman Airfuge ultracentrifuge for 10 min. For protease protection, translation products were digested with proteinase K (0.35 μg/μl) in the absence or presence of 1% Triton X-100 for 1 h on ice. Protease digestion was stopped with 10 mM phenylmethylsulfonyl fluoride. Samples were added to a 100-μl solution of 0.1 M Tris, 1% SDS (pH 8) and heated at 95 °C for 10 min.

**Deglycosylation, Immunoprecipitation, and Trichloroacetic Acid Precipitation**—Translation mixtures were centrifuged through a sucrose cushion, and pellets were solubilized in a solution containing 0.2% SDS, 100 mM sodium phosphate, 25 mM EDTA (pH 6.9) at 95 °C for 5 min. The samples were cooled to room temperature, diluted with 2% Triton X-100 in 100 mM sodium phosphate, 25 mM EDTA (pH 6.9), and digested with 0.1–1 μl of 1 units/μl PNGase F at 37 °C for the indicated times. [<sup>35</sup>S]-Labeled tyrosinase was immunoprecipitated with anti-tyrosinase antibodies (30). To determine radioactivity in total proteins, lysates were blotted on filter paper and treated with 10% trichloroacetic acid on ice for 30 min. Samples were washed with ice-cold 100% ethanol. The radioactivity of the blots was determined in a liquid scintillation counter.

**Calculation of TYR Concentration**—The approximate concentration of TYR in the *in vitro* translation reactions was determined as described below. Radioactive samples labeled with [<sup>35</sup>S]Met/Cys were fully resolved by SDS-PAGE to quantify the intensity of the translocated tyrosinase band by phosphorimaging. Equivalent samples were also loaded on the same gel after the run was 70% completed. Therefore, the samples were not resolved and the intensity of the total free label in the reaction could be determined. Because tyrosinase has a total of 28 Met and Cys, its approximate concentration is the following: [Tyr] = (T/F) × [Met/Cys]/28, where T is the intensity of the tyrosinase band and F is the intensity of the total free label. [Met/Cys] is the sum of the concentrations of endogenous reticulocyte lysate (3.9 μM) and the radioactive [<sup>35</sup>S]Met/Cys (0.9 μM).

**Metabolic Labeling of Tyrosinase**—Normal human melanocytes were cultured from newborn foreskins in Ham's F-10 medium supplemented with 7% fetal bovine serum and several ingredients required for their proliferation, including 12-O-tetradecanoylphorbol-13-acetate, 3-isobutyl-1-methylxanthine, dbcAMP (N<sup>6</sup>, 2'-O-dibutyryladenine 3, 5-cyclic monophosphate) and cholera toxin (43). Melanoma cells strains 501 mel and YUSIT1 were grown in Ham's F-10 medium plus serum (30). Cells were starved for 2 h in Met/Cys free-RPMI 1640 medium (supplemented with 3% dialyzed calf serum, 1% glutamine, 0.1 mM 3-isobutyl-1-methylxanthine, and 50 μg/ml 12-O-tetradecanoylphorbol-13-acetate), were then incubated with [<sup>35</sup>S]Met/Cys (0.7 mCi/ml) for 10 min, scraped into phosphate-buffered saline supplemented with 20 mM N-ethylmaleimide, and lysed in 2% CHAPS buffer. Cell extracts were immunoprecipitated with anti-tyrosinase antibodies (30).

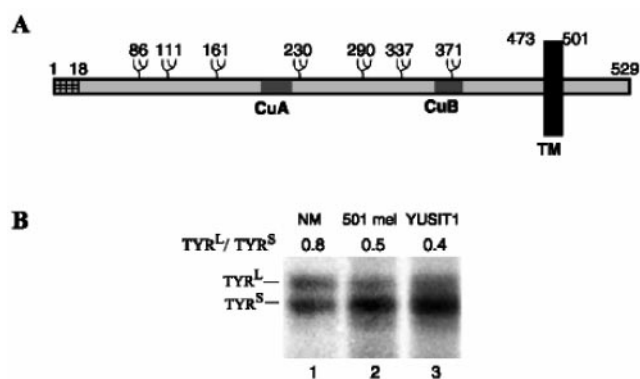


**FIG. 1. Topological map of human tyrosinase.** *A*, the 58-kDa tyrosinase includes an 18-amino acid signal sequence that directs the protein to the ER and a 29-amino acid cytosolic tail. Tyrosinase has seven putative glycosylation sites (*branched structures*) that increase its size to 70 kDa in the ER. It also contains two copper binding domains (*CuA* and *CuB*) that form a binuclear copper binding site. *B*, normal human melanocytes (*NM*) or melanoma cells (*501 mel* and *YUSIT1*) were pulsed with [<sup>35</sup>S]Met/Cys for 5 min. Tyrosinase was immunoprecipitated and resolved by SDS-PAGE and autoradiography. High and low molecular weight forms of tyrosinase are designated *TYR<sup>L</sup>* (large molecular weight) and *TYR<sup>S</sup>* (small molecular weight) respectively.

## RESULTS

**Translation and Translocation of Tyrosinase**—Newly synthesized tyrosinase from normal melanocytes migrated as a 70-kDa doublet band separated by ~3 kDa (Fig. 1*B*, lane 1) (30). An [<sup>35</sup>S]TYR doublet of similar mobility also accumulated in melanoma cells, but the intensities of the individual doublet bands varied. The ratio of the larger TYR to the smaller TYR in melanoma cells was half of that in normal melanocytes (0.4–0.5 compared with 0.8, respectively), indicating that the faster migrating form (*TYR<sup>S</sup>*) accumulated more predominantly in the melanoma cells.

To identify the cause of the TYR doublet, TYR was expressed in a cell-free system that facilitated experimental manipulation. The translation system consisted of rabbit reticulocyte lysate and mRNA encoding human TYR in the presence and absence of isolated RER membranes (Fig. 2). The native tyrosinase mRNA or a modified message termed *K<sup>b</sup>SS-TYR*, in which the TYR signal sequence was exchanged with the corresponding signal sequence from murine major histocompatibility complex class I molecule *K<sup>b</sup>* (*K<sup>b</sup>SS*) (40, 44), was used. A 60-kDa protein, recognized by anti-tyrosinase antibodies, was generated in the absence of microsomes that corresponded to untranslocated and unglycosylated TYR (Fig. 2, *A*, lanes 1 and 5, *U*TYR). However, a 70-kDa doublet identical to that observed previously in intact melanocytes (30) (Fig. 1*B*) accumulated in the presence of RER microsomes. This band represented translocated tyrosinase that had received multiple *N*-linked carbohydrates (Fig. 2*A*, lanes 3 and 7). The *K<sup>b</sup>SS-TYR* chimera was translated and translocated 4–6-fold more efficiently than native tyrosinase (Fig. 2*A*, compare lane 3 to lane 4). The untranslocated *K<sup>b</sup>SS-TYR* migrated slightly slower than wild type TYR (Fig. 2*A*, compare lane 1 to lane 2 and lane 5 to lane 6, *U*TYR) due to the different sizes of signal sequence (24 amino acids in *K<sup>b</sup>SS* and 18 amino acids in TYR). However, the mobility of the translocated products was identical (Fig. 2*A*, compare lane 3 to lane 4 and lane 7 to lane 8, *TYR*) and was similar to newly synthesized tyrosinase produced in intact melanocytes, justifying the use of the *K<sup>b</sup>SS-TYR* in all subsequent cell-free experiments.

The protein doublet constituted the translocated and glycosylated tyrosinase because it was precipitated with wheat germ agglutinin-bound beads (Fig. 2*B*, lane 4, *TYR*), and it sedimented through a sucrose cushion designed to isolate only

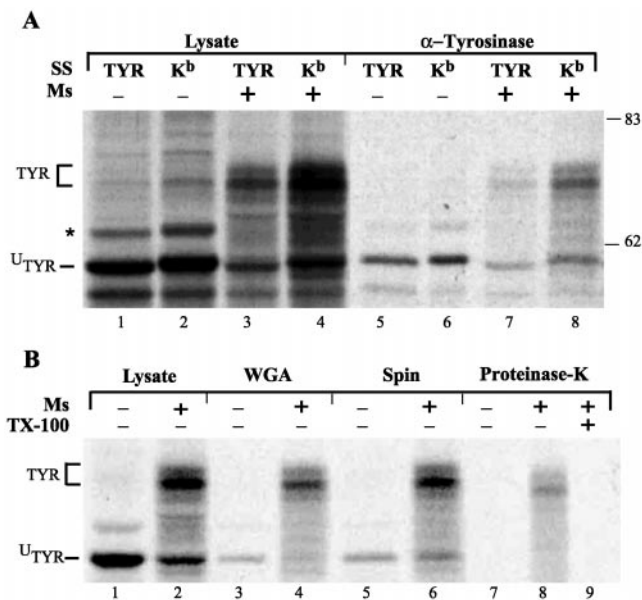


**FIG. 2. *In vitro* translation and translocation produces normally processed tyrosinase.** *A*, replacing the native 18-amino acid signal sequence (*SS*) of tyrosinase (MLLAVLYCLLWSFQTSAG) with the 24-amino acid murine major histocompatibility complex class I *K<sup>b</sup>SS* (MNSMVPCTLLLLLAAALAPTQTRG) increases efficiency of translation and translocation. Radiolabeled proteins synthesized in the presence or absence of RER microsomes (*Ms*) in the RRL translation system were resolved by 7.5% SDS-PAGE directly (lanes 1–4) or after immunoprecipitation with anti-tyrosinase antibodies (lanes 5–8). Molecular mass markers in kDa are indicated on the right, and translocated (*TYR*) and untranslocated (*U*TYR) bands are indicated on the left. \* denotes a RRL background band. *B*, the translocated doublet form of tyrosinase is a glycosylated protein. <sup>35</sup>S-Labeled tyrosinase was synthesized in the absence (lanes 1, 3, 5, and 7) or in the presence (lanes 2, 4, 6, 8, and 9) of microsomes with the RRL translation system. Samples were resolved directly, by SDS-PAGE (lanes 1 and 2), or after affinity precipitation with wheat germ agglutinin (*WGA*) (lanes 3 and 4). Alternatively, to assess translocation, the lysates were spun through a sucrose cushion, and the resuspended pellets were fractionated (lanes 5 and 6). Finally, digestion with proteinase K, which has access to untranslocated tyrosinase and to the cytoplasmic tail of the translocated protein, further demonstrated that TYR is correctly inserted into the ER microsomes (lanes 7–9).

membranes decorated with ribosomes (Fig. 2*B*, lane 6, *TYR*). Digestion with proteinase K degraded *U*TYR but not the *TYR* form, unless the microsomes were first solubilized by detergent (Fig. 2*B*, lanes 7–9). The downward mobility shift caused by proteinase K cleavage of the 29-amino acid cytosolic tail of the translocated form is consistent with correct insertion of the type I membrane protein into the microsomal membrane bilayer (Fig. 2*B*, compare lane 6 to lane 8, *TYR*). Taken together, the data supported the conclusion that the *in vitro* translated 70-kDa doublet represented ER translocated and glycosylated forms of tyrosinase.

**Tyrosinase Exists as Two Alternatively Processed *N*-Linked Core Glycans, *TYR<sup>7</sup>* and *TYR<sup>6</sup>***—The two translocated ER isoforms of tyrosinase could be generated by heterogeneous glucose or mannose trimming of *N*-linked glycans in the ER or through differential recognition by the OST generating differences in the total number of attached *N*-linked glycans. Differential trimming of glucose residues as the source for this variability was ruled out by the persistent production of doublet protein in the presence of DNJ, although the translated and processed products displayed slower mobility due to inhibition of glucosidases I and II activities (Fig. 3*A*, lanes 3 and 5). Likewise, differential ER carbohydrate trimming was excluded by the persistence of the doublet in the presence of the mannosidase inhibitor deoxymannojirimycin (data not shown).

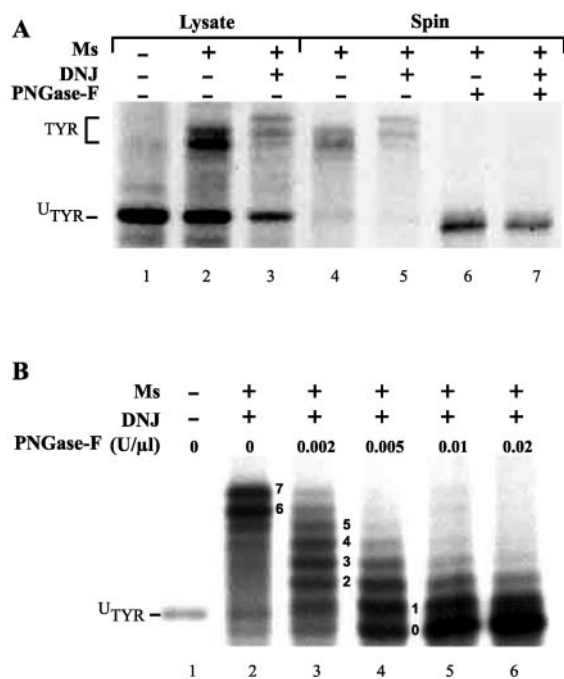


**FIG. 3. Tyrosinase doublet is due to differential glycosylation of tyrosinase by the OST.** A, [ $^{35}\text{S}$ ]TYR was translated under reducing conditions in the presence and absence of DNJ and microsomes. Translocated protein (TYR) was isolated from untranslocated ( $^{\text{U}}$ TYR) by ultracentrifugation and treated with PNGase F prior to resolution by SDS-PAGE. B, [ $^{35}\text{S}$ ]TYR was synthesized in the presence of DNJ using the RRL cell-free system. Limited digestion with varying concentrations of PNGase F produces a ladder of differentially glycosylated proteins. The numbers next to each band indicate the total number of glycans per tyrosinase molecule.

Heterogeneity in the carbohydrate side chains as the source of TYR doublet was indicated after digestion with the bacterial endoglycosidase PNGase F. This endoglycosidase removed all *N*-linked side chains coalescing the doublet into a single band that migrated slightly faster than the untranslocated form (Fig. 3A, lanes 6 and 7). The faster mobility of the PNGase F digested over the untranslocated form of tyrosinase (Fig. 3A, compare lanes 1 and 2 to lanes 6 and 7) was due to the cleavage of the signal sequence during RER processing. Therefore, we concluded that the doublet represented tyrosinase glycoforms with different numbers of *N*-linked glycans.

The number of glycans was then resolved by creating a ladder of partially cleaved PNGase F glycosidase products (Fig. 3B). Tyrosinase was produced in the presence of DNJ to eliminate variation due to glucose trimming. Complete digestion with high concentration of PNGase F generated an unglycosylated protein (Fig. 3B, lanes 4–6, band 0). However, PNGase F at lower concentrations produced a discrete ladder of eight bands corresponding to proteins with seven to zero glycans (Fig. 3B, lane 3; top and bottom bands, respectively). This analysis revealed that the doublet represented tyrosinase with seven (TYR<sup>7</sup>) and six (TYR<sup>6</sup>) *N*-linked glycans.

**Glycosylation of Asn-290 at the Consensus site Asn-Gly-Thr-Pro Is Suppressed by the Presence of Pro at Position 293**—The partial digestion by PNGase F suggested that the doublet was generated by inefficient glycosylation of one of the consensus sites. The smaller glycoform (TYR<sup>S</sup>) could be the product of site-specific inefficient glycosylation or random vacancy of any one of the sites. Glycosylation of a consensus site could be suppressed by inefficient transfer of truncated dolichol pyrophosphate precursors, competition with disulfide bond formation, or the presence of inefficient sites (45–48). The involvement of truncated dolichol pyrophosphate sugar precursor was

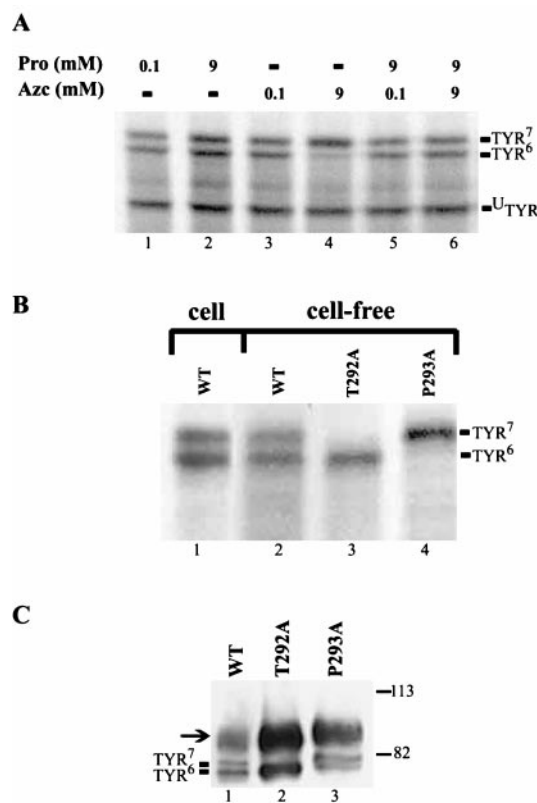


**FIG. 4. Pro-293 at the consensus glycosylation site (Asn-Gly-Thr-Pro) suppresses glycosylation.** A, [ $^{35}\text{S}$ ]TYR was translated under reducing conditions in the presence of varying concentrations of proline or the proline analogue Azc. B, mutant forms of tyrosinase, T292A and P293A, were translated along with wild type in the presence of RER microsomes under reducing conditions and subjected to SDS-PAGE and autoradiography. [ $^{35}\text{S}$ ]TYR in normal human melanocytes (*cell*) was synthesized with a 10-min pulse of [ $^{35}\text{S}$ ]Met/Cys, and the protein was immunoprecipitated with anti-tyrosinase antibodies prior to electrophoresis. C, *in vivo* processing of FLAG-tagged wild type (WT) and mutant tyrosinase proteins. Mouse melanocytes were harvested 1 week after transfection with plasmids encoding TYRwt-FLAG, TYR-T292A-FLAG, or TYR-P293A-FLAG. Cell lysates were subjected to immunoprecipitation with anti-tyrosinase antibodies and Western blotting with mAb against FLAG. The arrow designates the fully glycosylated forms of the chimeric proteins. Size markers are in kDa.

excluded because complete glycosylation of a variety of multi-glycosylated substrates has been reported with this cell-free system (14, 49, 50), and the doublet appeared in cells. Furthermore, we ruled out competition by disulfide bond formation, because the doublet persisted even when tyrosinase was synthesized in the presence of the reducing agent dithiothreitol (Fig. 2 and data not shown).

A clue that a proline residue had a role in the hypoglycosylation came from experiments using the proline analogue azetidine-2-carboxylic acid (Azc). Although the doublet persisted when tyrosinase was synthesized in the presence of equal molar Azc and proline (Fig. 4A, lane 6), hypoglycosylation was arrested, and complete glycosylation to TYR<sup>7</sup> was observed with an excess of Azc (Fig. 4A, lane 4). These results suggested that a proline located proximal to the hypoglycosylated site was involved in the hypoglycosylation of TYR<sup>6</sup>.

A scan of the human tyrosinase amino acid sequence revealed a Pro immediately downstream from the Asn-290 consensus glycosylation sequence (Asn-Gly-Thr-Pro-293). To determine whether hypoglycosylation of Asn-290 was the source of the doublet, this glycosylation site was removed by substituting Thr with an Ala at position 292 (TYR-T292A). *In vitro* translation of TYR-T292A produced a single band with mobility

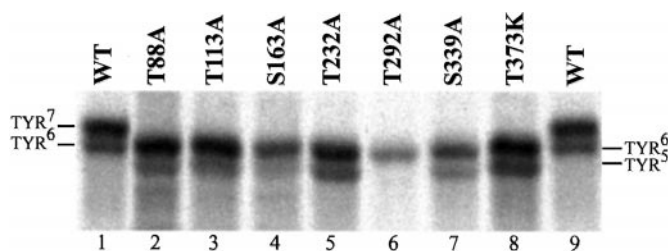


**FIG. 5. All seven glycans in tyrosinase are processed.** All seven putative *N*-linked glycosylation sites were eliminated individually by mutation of the consensus site (Thr/Ser to an Ala, or in the case of Thr-373 to a Lys). [<sup>35</sup>S]TYR was translated with the RRL system in the presence of semi-permeabilized melanocyte prior to resolution by reducing SDS-PAGE.

equivalent to TYR<sup>6</sup> (Fig. 4B, lane 3). In contrast, a single band with mobility of TYR<sup>7</sup> was produced when Pro-293 was exchanged for an Ala (TYR-P293A) (Fig. 4B, lane 4). Likewise, *in vivo* synthesis of FLAG-tagged wild type and mutant tyrosinase proteins transiently expressed in mouse melanocytes produced similar results (Fig. 4C). In the latter case, the differences in the migration pattern was restricted to the ER form, as all ectopically expressed proteins possessed Golgi processed complex carbohydrates and matured normally (Fig. 4C, arrow). Because the mutant TYR-P293A was completely glycosylated, we concluded that the proximal proline at position 293 was the source of tyrosinase hypoglycosylation.

The utilization of the other six consensus *N*-linked glycosylation sites was confirmed by site directed mutagenesis. Here, *in vitro* translated proteins were translocated into the ER of semi-permeabilized melanocytes. As observed with the RER microsomes, the wild type protein migrated as a protein doublet (Fig. 5, lane 1). Consistent with the results obtained by PNGase F partial digestion (Fig. 3B), exchanging the Thr or Ser of each of the seven consensus sites with Ala (or Lys in the case of Thr-373) induced an identical downward mobility shift of TYR (Fig. 5, lanes 2–8). The T373K mutation was utilized here, because it is a common human mutation that causes albinism due to the retention of the protein in the ER (31). It should also be noted that a doublet was produced with all mutants excluding T292A.

**Glycosylation of Asn-290 Is More Efficient at Slow Rates of Translation**—The intensity of the individual bands of the doublet was dependent on the translation system employed, as the ratio of TYR<sup>7</sup>/TYR<sup>6</sup> was 0.77 in the wheat germ translation system and 0.50 or smaller in the RRL (Fig. 6A, lanes 1 and 2). These two systems also displayed differences in translation times. The translation time for tyrosinase was 15 min with the WG and 10 min with the RRL system (Fig. 6B, as determined by the *x* intercept). These translation times at 27 °C corresponded to translation rates of 0.6 and 0.9 amino acids/s in WG and RRL, respectively. Therefore, we explored the possibility that rapid translation rates contributed to hypoglycosylation of tyrosinase at the Asn-290 site.

Toward this aim, the protein synthesis inhibitor cycloheximide (CHX) was employed. Although CHX blocks protein synthesis at concentrations above 100 μM, it only slows translation at lower concentrations (7). Indeed, slowing the translation time of tyrosinase in the RRL system to 20 min with 0.3 μM CHX increased the ratio of TYR<sup>7</sup>/TYR<sup>6</sup> to 0.71 (Fig. 6A, lane 3, and Fig. 6B, RRL + CHX), indicating an increase in the level of glycosylation. Higher concentration of CHX resulted in additional decrease in translation rate, further increasing glycosylation (Fig. 6A, lane 4). Therefore, we concluded that the suppressive effect of Pro on glycosylation at the Asn-Gly-Thr-Pro consensus site was alleviated when the rate of translation was reduced.

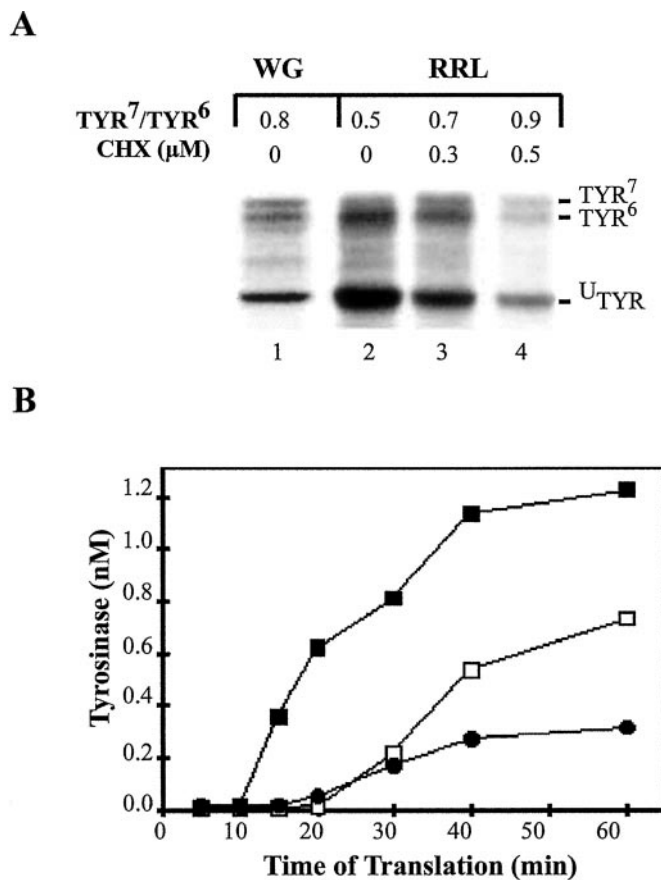


**FIG. 6. Translation rate affects glycosylation efficiency of Asn-Gly-Thr-Pro.** A, [<sup>35</sup>S]TYR was translated under reducing conditions with either a WG or RRL translation system in the presence of varying concentrations of CHX and resolved by SDS-PAGE. The TYR<sup>7</sup>/TYR<sup>6</sup> ratio was calculated after the quantification of the radioactive protein bands by phosphorimaging. B, amount of translocated tyrosinase (TYR<sup>6</sup> + TYR<sup>7</sup>) versus the time of translation in RRL (filled squares), in RRL with 0.3 μM CHX (open squares), or in WG (circles). The *x* intercept of the curves approximates the total synthesis time of full-length tyrosinase under the different conditions.

**Cellular Translation Rates**—We went on to determine whether the difference in glycosylation levels of tyrosinase in normal melanocytes versus melanoma cells was due to differences in translation rates. Translation rates were determined by performing short radioactive pulses with [<sup>35</sup>S]Met/Cys, followed by the quantification of TYR levels. Half-times of synthesis were determined as the *x* intercept of the plot of TYR level versus pulse time (Fig. 7), minus the time for general radiolabel incorporation into the cells determined by trichloroacetic acid precipitation (data not shown) (7, 51, 52).

The synthesis time of TYR in normal melanocytes was 2.53 min (3.5 amino acids/s), compared with 1.15 (7.7 amino acids/s) and 0.89 min (10.0 amino acids/s) (Fig. 7B) in the amelanotic melanoma cell lines 501 mel and YUSIT1, respectively. As seen earlier in the cell-free system, the slower rate of TYR translation corresponded to a higher level of TYR<sup>7</sup> (Fig. 7A, compare lanes 1–5 to lanes 6–16). Moreover, slowing the rate of translation in melanoma cells with 1 or 10 μM CHX to 3.4 and 8.1 min, respectively, permitted more complete glycosylation to TYR<sup>7</sup> (Fig. 8), as seen before in the cell-free system. This was accompanied by a dramatic increase in the glycosylation of TYR, as reflected by an increase in the ratio of TYR<sup>7</sup>/TYR<sup>6</sup> from 0.4 to 1.7 in the presence of 10 μM CHX. Therefore, the rate of TYR translation influenced the glycosylation profiles of TYR synthesized in the cell-free system and in live cells. However, slowing the translation rate by decreasing the temperature had

FIG. 7. Synthesis time of tyrosinase.

A, normal melanocytes and melanoma cells (501 mel and YUSIT1) were pulsed with [<sup>35</sup>S]Met/Cys for the times indicated. The lysates were immunoprecipitated with α-TYR, subjected to SDS-PAGE, and quantified by phosphorimager analysis. B, [<sup>35</sup>S]TYR levels were plotted versus the time of the radioactive pulse. Radioactivity in trichloroacetic acid precipitates of each sample was determined with a liquid scintillation counter (data not shown). The x intercepts of the [<sup>35</sup>S]TYR and the trichloroacetic acid precipitation plots fitted by a straight line were subtracted from each other. This value is equal to the half-time of synthesis (7, 51). For calculated values, see Table I.

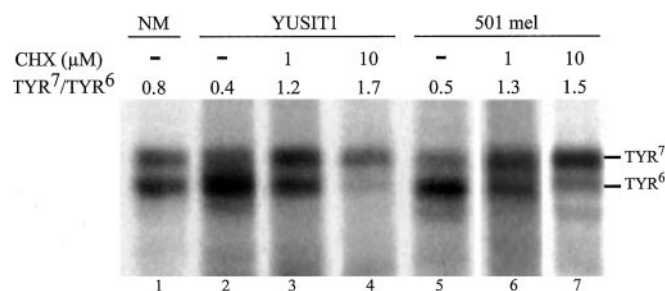
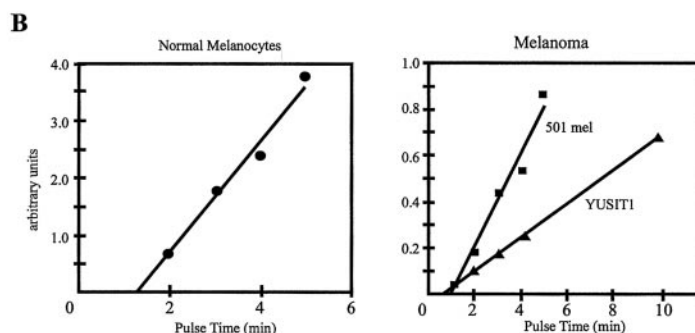
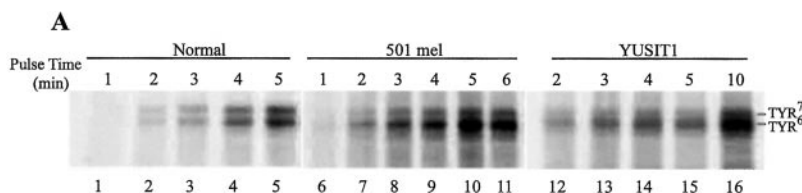


FIG. 8. Translation rate determines glycosylation efficiency in melanocytes. Normal melanocytes (NM) and melanoma cells (YUSIT1 and 501 mel) were pulsed with [<sup>35</sup>S]Met/Cys in the absence of CHX (–) for 5 min or in the presence of 1 and 10 μM CHX for 10 and 20 min, respectively. The lysates were immunoprecipitated with α-TYR and resolved by SDS-PAGE and autoradiography. TYR<sup>7</sup>/TYR<sup>6</sup> ratios were determined by phosphorimaging.

no effect on the TYR<sup>7</sup>/TYR<sup>6</sup> ratio, likely due to the glycan transfer reaction also being slowed (data not shown).

Similar analysis was performed with two other proteins to determine whether the difference in the rate of TYR synthesis between normal melanocytes and melanoma cells was general or protein specific (Table I). The results show similar synthesis times for calnexin and tyrosinase-related protein 1 (TRP1) in the two melanoma cells and normal melanocytes. This indicated that the decreased translation rate observed in normal melanocytes was specific to tyrosinase.

#### DISCUSSION

The important role of the ER quality control system in the maturation of tyrosinase has been observed in normal and malignant melanocytes (30). In normal human melanocytes, tyrosinase slowly reaches the Golgi, with a half-time of ~1.5 h, while most of the wild type protein in amelanotic melanoma cells is retained in the ER and is then targeted for degradation by the ubiquitin-dependent cytosolic proteasomal system. To further understand this critical quality control process, we have investigated the maturation of human tyrosinase in normal melanocytes, melanoma cells, semipermeabilized cells, and a cell-free system. The cell-free system reproduced the early stages of maturation in the ER and permitted the detailed analysis of tyrosinase translocation and glycosylation. Furthermore, it helped resolve the nature of human tyrosinase early glycoforms that appeared as a doublet in melanocytes.

TABLE I  
Synthesis times for proteins in normal melanocytes and melanoma cells

Cells/protein	Synthesis time		
	TYR	TRP1	Calnexin
		<i>min</i>	
Normal melanocytes	2.53 ± 0.17	0.74	1.01 ± 0.16
Melanoma 501 mel	1.15 ± 0.03	0.67 ± 0.10	1.15 ± 0.07
Melanoma YUSIT1	0.89 ± 0.19	NA <sup>a</sup>	1.18 ± 0.01

<sup>a</sup> NA, not applicable because TRP1 is not expressed in YUSIT1.

Upon translocation into the lumen of the ER, tyrosinase cotranslationally received multiple *N*-linked glycans, resulting in a 12-kDa gain in molecular mass. Limited PNGase F digestion and site-directed mutagenesis showed that all consensus sites are being utilized and that the doublet ER translocated form represents a protein with six or seven glycans. We found that the source of the heterogeneity was the inefficient recognition by the OST of Asn-290 (Asn-Gly-Thr-Pro). Interestingly, mouse tyrosinase lacks the inefficient glycosylation site at Asn-290 but retains the remaining six observed in the human protein. However, unlike human tyrosinase, the second and third sites in the mouse counterpart (Asn-111 and Asn-161) were reported to be unrecognized, producing a protein with only four glycans (53).

Hypoglycosylation at Asn-290 of human tyrosinase occurred during *in vivo* and cell-free processing based on the following observations. 1) Partial digestion of tyrosinase with PNGase F showed that the upper and lower bands of the doublet corresponded to tyrosinase with seven and six processed glycans, termed TYR<sup>7</sup> and TYR<sup>6</sup>, respectively, indicating inefficient glycosylation of a single site. 2) Substituting Pro with its analogue Azc during translation of tyrosinase produced more efficient glycosylation, identifying a role for Pro in the hypoglycosylation. Indeed, a Pro is located immediately carboxyl to the glycosylation site of Asn-290 (Pro-293). 3) Mouse tyrosinase has six consensus glycosylation sites, lacking the one corresponding to Asn-290 in human tyrosinase (33, 34, 36). Consistent with this difference, the early glycoform of mouse tyrosinase migrates in SDS-PAGE as a protein singlet (54), whereas early glycoforms of human tyrosinase produced in normal melanocytes appear as a doublet (Fig. 1B and Ref. 30). 4) The substitution of Pro-293 with an Ala in human TYR produced a single protein band that migrated with mobility corresponding to

TYR<sup>7</sup>. 5) Likewise, abolishing the glycosylation site at Asn-290 with an Ala at position 292 produced a single protein band that corresponded to TYR<sup>6</sup>. Together, our results support the conclusion that the source for tyrosinase hypoglycosylation is the inefficient recognition of Asn-290 by the OST due to suppression by Pro-293.

Proline suppresses glycan transfer to the consensus site Asn-X-(Thr/Ser)-Y when found in the X position (55). However, its effect on glycosylation when in other proximal locations is poorly understood. Sites that have a Pro in the Y position often go unrecognized by the OST (46), as well as by many of the protein analysis software programs used to identify potential glycosylation sites in a primary amino acid sequence. Protein heterogeneity caused by Pro suppression of glycosylation is likely to be found for a large range of glycoproteins.

The efficiency of glycosylation of Asn-Gly-Thr-Pro correlated inversely with the rate of translation. The fully glycosylated TYR<sup>7</sup> species was produced more efficiently when tyrosinase was translated in the slower translation systems (cell-free WG system or normal melanocytes), as well as in the RRL translation system and melanoma cells, both of which were slowed by CHX. A tight window for cotranslational glycosylation exists shortly after the consensus sequence enters the ER lumen, determined by the position of the OST active site 30–40 Å, or 12–14 residues from the membrane into the lumen of the ER (11). Therefore, slowing down the rate of translation may maintain the inefficient Asn-290-Gly-Thr-Pro glycosylation site in human tyrosinase in proximity to the OST active site for sufficient time to allow glycosylation.

In addition to the precise distance from the membrane, recognition by the OST may also have conformational requirements. It appears that transfer entails roughly a parallel configuration of the Asn-X-(Thr/Ser) sequence in relation to the ER membrane (46). Therefore, it is likely that in the context of the full-length protein, interference by Pro proximal to the Asn-290 consensus site decreases the probability that the consensus sequence attains the correct orientation that permits transfer of the glycan to the inefficient site.

The level of glycosylation did not appear to influence the ability of tyrosinase to exit the ER as both TYR<sup>6</sup>-FLAG and TYR<sup>7</sup>-FLAG obtained complex glycans in the Golgi as indicated by the appearance of 90-kDa forms. These results were confirmed by direct visualization of TYR and GFP chimeras (TYR<sup>6</sup>-GFP and TYR<sup>7</sup>-GFP) in the cell periphery, indicative of melanosomal localization (data not shown). It remains to be determined whether having the additional glycan confers any maturational or functional advantage.

The translation rate of tyrosinase synthesized in normal melanocytes was slower than that found in the melanoma cell lines. However, the rates of translation of TRP1, a protein homologous to tyrosinase, and the ER molecular chaperone calnexin were similar in both cell types. Why the translation of TYR in normal melanocytes is slowed compared with other proteins in both normal melanocytes and melanoma cells remains to be determined. Because the protein is wild type in both cell systems (30), the differential regulation of translation cannot involve differences in the TYR gene. Furthermore, RT-PCR analysis demonstrated that TYR mRNA was 2–3-fold more abundant in normal melanocytes compared with melanoma cells, excluding the possibility that high message levels caused the faster translation rate in melanoma cells (data not shown).

The folding state of a protein in the ER can be communicated to the translation machinery through the unfolded protein response. Here, during times of stress when large concentrations of unfolded proteins have accumulated in the ER and the

unfolded protein response is turned on, the ER membrane kinase PERK phosphorylates eIF2- $\alpha$ , causing the inhibition of translation initiation (56, 57). Another known mode of translation regulation involves the phosphorylation of elongation factor eEF2 by cAMP-dependent kinase that decreases the rate of protein elongation (58). Although differences in the initiation rates in normal melanocytes *versus* melanoma cells cannot be discounted, the root of the variation is likely to be the elongation step, because TYR mRNA levels were higher in normal melanocytes (data not shown), and treatment of melanoma cells with low concentrations of cycloheximide recapitulated the normal melanocyte glycosylation pattern. The involvement of a nonspecific mechanism of translational regulation known to affect all proteins in a similar manner was also ruled out by the observations that synthesis times of calnexin and TRP1 were the same in normal melanocytes and melanoma cells.

Ribosomal or translational pausing has been implicated in signal recognition particle-dependent targeting to the ER membranes, helping to ensure efficient targeting (59). Translational control has also been demonstrated to occur during the translocation of apolipoprotein B100 across the ER membrane, dependent upon the availability of newly synthesized lipids (60), and during the synthesis of the membrane-bound chloroplast reaction center protein D1, which is hypothesized to facilitate the cotranslational binding of its cofactors (61). Translational control could also play an important role in the vectorial folding of sequential folding domains and other cotranslational maturation events including glycosylation. Revealing the components in the translation system that regulate translation and influence tyrosinase maturation may provide important insights into our understanding of why wild type tyrosinase is targeted for degradation in melanoma cells, and may offer a more general explanation for other phenotypes associated with cancerous cells.

**Acknowledgments**—We thank Drs. J. Huppa and H. Ploegh (Boston, MA) for the pSP72/K<sup>b</sup>SS-CD3 $\delta$  plasmid, Dr. R. Spritz (Denver, CO) for the human tyrosinase cDNA pcTYR, and Dr. R. Gilmore (Worcester, MA) for RER microsomes. We acknowledge Robert Daniels for help with the construction of glycosylation mutations, Sherri Svedine with the confocal microscopy, and Dr. Sergio Trombetta and members of the Hebert laboratory for their thoughtful discussions.

#### REFERENCES

- Chen, W., Helenius, J., Braakman, I., and Helenius, A. (1995) *Proc. Natl. Acad. Sci. U. S. A.* **92**, 6229–6233
- Frydman, J., Erdjument-Bromage, H., Tempst, P., and Hartl, F. U. (1999) *Nat. Struct. Biol.* **6**, 697–705
- Molinari, M., and Helenius, A. (2000) *Science* **288**, 331–333
- Feldman, D. E., and Frydman, J. (2000) *Curr. Opin. Struct. Biol.* **1**, 26–33
- Netzer, W. J., and Hartl, F. U. (1997) *Nature* **388**, 343–349
- Bergman, L. W., and Kuehl, W. M. (1979) *J. Biol. Chem.* **254**, 5690–5694
- Braakman, I., Hoover-Litty, H., Wagner, K. R., and Helenius, A. (1991) *J. Cell Biol.* **114**, 401–411
- Molinari, M., and Helenius, A. (1999) *Nature* **402**, 90–93
- Frandsen, R., Cuozzo, J. W., and Kaiser, C. A. (2000) *Trends Cell Biol.* **10**, 203–210
- Kornfeld, R., and Kornfeld, S. (1985) *Annu. Rev. Biochem.* **54**, 631–664
- Nilsson, I., and von Heijne, G. (1993) *J. Biol. Chem.* **268**, 5798–5801
- Ou, W.-J., Cameron, P. H., Thomas, D. Y., and Bergeron, J. J. M. (1993) *Nature* **364**, 771–776
- Hammond, C., Braakman, I., and Helenius, A. (1994) *Proc. Natl. Acad. Sci. U. S. A.* **91**, 913–917
- Hebert, D. N., Foellmer, B., and Helenius, A. (1995) *Cell* **81**, 425–433
- Peterson, J. R., Ora, A., Van, P. N., and Helenius, A. (1995) *Mol. Biol. Cell* **6**, 1173–1184
- Van Leeuwen, J. E. M., and Kearsse, K. P. (1996) *Proc. Natl. Acad. Sci. U. S. A.* **93**, 13997–14001
- Rajagopalan, S., Xu, Y., and Brenner, M. B. (1994) *Science* **263**, 387–390
- Hebert, D. N., Foellmer, B., and Helenius, A. (1996) *EMBO J.* **15**, 2961–2968
- Vassilakos, A., Cohen-Doyle, M. F., Peterson, P. A., Jackson, M. R., and Williams, D. B. (1996) *EMBO J.* **15**, 1495–1506
- Varki, A. (1993) *Glycobiology* **3**, 97–130
- Helenius, A. (1994) *Mol. Biol. Cell* **5**, 253–265
- Ellgaard, L., Molinari, M., and Helenius, A. (1999) *Science* **286**, 1882–1888
- Lerner, A. B., Fitzpatrick, T. B., Calkins, E., and Summerson, W. H. (1949) *J. Biol. Chem.* **178**, 185–195
- Körner, A., and Pawelek, J. (1982) *Science* **217**, 1163–1165
- Tripathi, R. K., Hearing, V. J., Urabe, K., Aroca, P., and Spritz, R. A. (1992)

- J. Biol. Chem.* **267**, 23707–23712
26. Kantheti, P., Qiao, X., Diaz, M. E., Peden, A. A., Meyer, G. E., Carskadon, S. L., Kapfhamer, D., Sufalko, D., Robinson, M. S., Noebels, J. L., and Burmeister, M. (1998) *Neuron* **21**, 111–122
  27. Feng, L., Seymour, A. B., Jiang, S., To, A., Peden, A. A., Novak, E. K., Zhen, L., Rusiniak, M. E., Eicher, E. M., Robinson, M. S., Gorin, M. B., and Swank, R. T. (1999) *Hum. Mol. Genet.* **8**, 323–330
  28. Dell'Angelica, E. C., Shtetlersuk, V., Aguilar, R. C., Gahl, W. A., and Bonifacino, J. S. (1999) *Mol. Cell* **3**, 11–21
  29. Spritz, R. A. (1999) *Trends Genet.* **15**, 337–340
  30. Halaban, R., Chang, E., Zhang, Y., Moellmann, G., Hanlon, D., Michalak, M., Setaluri, V., and Hebert, D. N. (1997) *Proc. Natl. Acad. Sci. U. S. A.* **94**, 6210–6215
  31. Halaban, R., Svedine, S., Cheng, E., Aron, R., and Hebert, D. N. (2000) *Proc. Natl. Acad. Sci. U. S. A.* **97**, 5889–5894
  32. Petrescu, S. M., Branza-Nichita, N., Negroiu, G., Petrescu, A. J., and Dwek, R. A. (2000) *Biochemistry* **39**, 5229–5237
  33. Kwon, B. S., Haq, A. K., Pomerantz, S. H., and Halaban, R. (1987) *Proc. Natl. Acad. Sci. U. S. A.* **84**, 7473–7477
  34. Ruppert, S., Muller, G., Kwon, B., and Schutz, G. (1988) *EMBO J.* **7**, 2715–2722
  35. Bouchard, B., Fuller, B. B., Vijayasaradhi, S., and Houghton, A. N. (1989) *J. Exp. Med.* **169**, 2029–2042
  36. Yamamoto, H., Takeuchi, S., Kudo, T., Sato, C., and Takeuchi, T. (1989) *Jpn. J. Genet.* **64**, 121–135
  37. Oetting, W. S., and King, R. A. (1999) *Hum. Mutat.* **13**, 99–115
  38. King, R. A. (1998) *The Pigmentary System. Physiology and Pathophysiology*, 1st Ed. (Nordlund, J. J., Boissy, R., Hearing, V. J., King, R. A., and Ortonne, J.-P., eds.) Oxford University Press, New York
  39. Berson, J. F., Frank, D. W., Calvo, P. A., Bieler, B. M., and Marks, M. S. (2000) *J. Biol. Chem.* **275**, 12281–12289
  40. Huppa, J. B., and Ploegh, H. L. (1997) *J. Exp. Med.* **186**, 393–403
  41. Bennett, D. C., Cooper, P. J., Dexter, T. J., Devlin, L. M., Heasman, J., and Nester, B. (1989) *Development* **105**, 379–385
  42. Wilson, R., Allen, A. J., Oliver, J., Brookman, J. L., High, S., and Bulleid, N. J. (1995) *Biochem. J.* **307**, 679–687
  43. Böhm, M., Moellmann, G., Cheng, E., Alvarez-Franco, M., Wagner, S., Sassone-Corsi, P., and Halaban, R. (1995) *Cell Growth Differ.* **6**, 291–302
  44. Bijlmakers, M. J., Neeffjes, J. J., Wojcik-Jacobs, E. H. M., and Ploegh, H. (1993) *Eur. J. Immunol.* **23**, 1305–1313
  45. Turco, S. J., Stetson, B., and Robbins, P. W. (1977) *Proc. Natl. Acad. Sci. U. S. A.* **74**, 4411–4414
  46. Gavel, Y., and von Heijne, G. (1990) *Protein Eng.* **3**, 433–442
  47. Allen, S., Naim, H. Y., and Bulleid, N. J. (1995) *J. Biol. Chem.* **270**, 4797–4804
  48. Holst, B., Bruun, A. W., Kielland-Brandt, M. C., and Winther, J. R. (1996) *EMBO J.* **15**, 3538–3546
  49. Cannon, K. S., Hebert, D. N., and Helenius, A. (1996) *J. Biol. Chem.* **271**, 14280–14284
  50. Hebert, D. N., Zhang, J.-X., Chen, W., Foellmer, B., and Helenius, A. (1997) *J. Cell Biol.* **139**, 613–623
  51. Horwitz, M. S., Scharff, M. D., and Maizel, J. J. V. (1969) *Virology* **39**, 682–694
  52. Fan, H., and Penman, S. (1970) *J. Mol. Biol.* **50**, 655–670
  53. Branza-Nichita, N., Negroiu, G., Petrescu, A. J., Garman, E. F., Platt, F. M., Wormald, M. R., Dwek, R. A., and Petrescu, S. M. (2000) *J. Biol. Chem.* **275**, 8169–8175
  54. Halaban, R., Pomerantz, S. H., Marshall, S., and Lerner, A. B. (1984) *Arch. Biochem. Biophys.* **230**, 383–387
  55. Marshall, R. D. (1972) *Annu. Rev. Biochem.* **41**, 673–702
  56. Harding, H. P., Zhang, Y., and Ron, D. (1999) *Nature* **397**, 271–274
  57. Harding, H. P., Zhang, Y., Bertolotti, A., Zeng, H., and Ron, D. (2000) *Mol. Cell* **5**, 897–904
  58. Hovland, R., Eikhom, T. S., Proud, C. G., Cressey, L. I., Lanotte, M., Doskeland, S. O., and Houge, G. (1999) *FEBS Lett.* **444**, 97–101
  59. Wolin, S. L., and Walter, P. (1988) *EMBO J.* **7**, 3559–3569
  60. Pan, M., Liang, J., Fisher, E. A., and Ginsberg, H. N. (2000) *J. Biol. Chem.* **275**, 27399–27405
  61. Kim, J., Klein, P. G., and Mullet, J. E. (1991) *J. Biol. Chem.* **266**, 14931–14938